INSPIRE:
Investigating Stellar Population In REIics
Data Release 2 (DR2)

C. Spiniello[1,2], L. Coccato[3], G. D'Ago[4], C. Tortora[2]
& the INSPIRE Team

[1]Sub-Dep. of Astrophysics, University of Oxford, Denys Wilkinson Building, Keble Road, Oxford, UK
[2]INAF - Osservatorio Astronomico di Capodimonte, Salita Moiariello, 16, I-80131 Napoli, Italy
[3]European Southern Observatory, Karl-Schwarzschild-Strasse 2, 85748, Garching, Germany
[4]Institute of Astrophysics, Pontificia Universidad Católica de Chile, Av. Vicuna Mackenna 4860, 7820436 Macul, Santiago, Chile

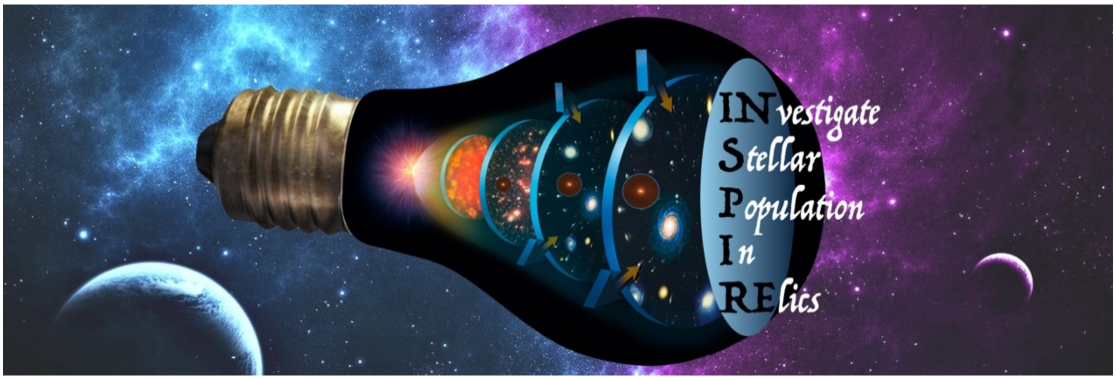

Abstract

This document describes the second public data release (DR2) of the X-Shooter ESO Large Program 1104.B-0370, "INvestigating Stellar Population In Relics (INSPIRE), which is firstly introduced in the INSPIRE pilot project (Spiniello et al., 2021a, A&A, 646, A28, hereafter S21a).

The first data release, published in March 2021, and described in the accompanying paper Spiniello et al. 2021b (A&A, 654, A136 hereafter S21b), comprised of 19 ultra-compact massive galaxies for which integrated stellar velocity dispersion, as well as mass-weighted age and metallicity and light-weighted [Mg/Fe] had been precisely measured. In this DR2 we release one-dimensional (1D) spectra in the UVB and VIS and NIR arms, of 21 additional systems, for which ESO observation have been completed before March 2022. Also in this case, we accompanied the DR with a scientific paper (D'Ago et al., 2022, **arXiv:2302.05453**.) that focusses on measuring the velocity dispersion from 1D spectra and assessing the systematics on it. In addition, we release again the spectra for the 19 objects described in DR1 and S21b, adding this time also the NIR arm.

Scientific Context

The first generation of extremely massive Early-Type Galaxies (ETGs) is already in place at $z \geq 3$ (Guo et al., 2013); their number density dramatically increases between $3 < z < 1$ (Trujillo et al. 2007) and then only mildly evolves at $z < 1$ (Bell et al. 2003). Interestingly, at higher redshift, massive red objects are found to have 3–5 times smaller sizes than in the local Universe, and thus they are 30–100 times denser (van Dokkum et al., 2008).

To reconcile these observations, a *two-phase formation scenario* (Oser et al., 2010) has been proposed to explain the mass assembly and evolution across cosmic time of very massive galaxies. A first intense and fast dissipative series of processes form their central "bulk" mass (at z>2) generating, after star formation quenches, a massive, passive and very compact galaxy with size a factor of ~4 smaller than local massive galaxies (the so-called "red nuggets", Daddi et al. 2005). Then a second, more time-extended phase, dominated by mergers and gas inflows, is responsible for the dramatic structural evolution and size growth from z~1 to today (Buitrago et al., 2008). Unfortunately, this "accreted" material overlaps, along the line-of-sight, with the spatial and orbital distributions of the "in-situ" light, that encodes the information about high-z baryonic processes, irreversibly limiting our resolving power. Luckily, since merging is believed to be stochastic, a small fraction of red nuggets survives intact until the local Universe, without experiencing any further interaction: **Relic Galaxies**. *Relics are the perfect local "laboratories" to study the processes that shaped the mass assembly of massive galaxies in the high-z Universe and disentangle between possible formation scenarios for massive galaxies*.

In the local Universe, only three relics have been confirmed and studied in great details (Trujillo et al. 2014, Ferré-Mateu et al., 2017, hereafter F17). They have large rotation velocities (~200-300 km/s) and high central stellar velocity dispersions (>300 km/s). From a stellar population point of view, these three objects have a single stellar population with super-solar metallicities and old ages out to several effective radii. Their stars are also characterized by a large [Mg/Fe] over-abundance, which is consistent with early and short star formation episodes (within timescales < 1 Gyr, Thomas et al. 2005). Finally, the three relics also have a bottom-heavy stellar initial mass function (IMF), with the fraction of low-mass stars being at least a factor of 2 larger than that found in the Milky Way (F17).

The goal of INSPIRE is to build the first catalogue of spectroscopically confirmed relics at 0.1<z<0.5, bridging the gap between the three local confirmed relics and the high-z red nuggets, to understand the discrepancy between the observational results and to put a stringent constraint on the predictions from simulations. A more detailed descriptions of the scientific aims and goal of INSPIRE is provided in S21a and S21b, where we also present results obtained using data released here.

According to the definition given in Tortora et al. (2016), a galaxy is defined as UCMG if it has an effective radius $R_{eff} < 1.5$ kpc and a stellar mass $M_* > 8 \times 10^{10}$ M_{sun}. However, since different studies have adopted different thresholds for size and masses, and since we aim at finding a large number of relics, we slightly relax these criteria and consider as confirmed UCMGs all objects with $R_{eff} < 2$kpc and stellar masses $M_* > 6 \times 10^{10}$ M_{sun}. .

Overview on INSPIRE

INSPIRE is based on data obtained as part of the ESO Large Programme ID: 1104.B-0370, PI: C. Spiniello, which has been awarded 154 hrs of observations on X-Shooter to spectroscopically follow up 52 UCMGs with redshift 0.1<z<0.5, which are part of a dedicated KiDS project (Tortora et al. 2018, Scognamiglio et al. 2020). Details on the target selections, observation strategy for the whole INSPIRE Programme were already given in the release description of the first DR. We summarise the most important ones here below.

Selection of the targets

The targets have been selected from multi-band imaging from the Kilo Degree Survey (KiDS) project, thanks to a project specifically dedicated to the search for Ultra-Compact Massive Galaxies (UCMGs) at redshift z<0.5 (T16, Tortora et al. 2018, Scognamiglio et al. 2020, hereafter T18 and S20).

About 100 of the photometrically selected candidates were also spectroscopically confirmed. Among these, INSPIRE targets the 52 objects with *g-i* broad band colour compatible with that of a stellar population with integrated age larger than 8 Gyrs, considering a solar, super-solar and a sub-solar metallicity (Fig. 1, in S21b).

Each galaxy has structural parameters computed from *gri* KiDS images (Roy et al. 2018) and stellar masses retrieved from T18/S20.

Observation Strategy and current status

The observation strategy has been optimized to capitalize on relatively sub-standard observing conditions (seeing up to 1.2, CLR nights, grey lunar phase with Moon FLI<0.5), allowing for an easy schedulability of the objects into the observation queue. Moreover, the selected targets span a very wide range in right ascension (RA) and declination (DEC), as can be seen from the histograms below, with an optimum observing time spread over the full year. This makes service mode observations, under a LP highly efficient. We note also that we have many systems with declination <-30, perfect as "fillers" in nights with strong wind coming from the North.

The slit widths is always 1.6 arcsec in the UVB and 1.5 in VIS and NIR to ensure minimal slit loss. A dithering scheme (NODDING MODE) with multiple frames where the galaxy is offset by a small amount from the center of the slit is used to facilitate a proper sky subtraction. Finally, we also implement a sigma clipping routine to further clean the 2D spectra from cosmic ray and sky residuals. Similarly to DR1, the seeing during the observations ranged between 0.85 to 1.2 arcsec, with a median value of ~1". We note that the spectra are fully seeing-dominated, as the effective radii of all objects in arcseconds (apparent sizes, on average Reff~0.3-0.4") are much smaller than the median seeing of the observations.

The final integration time on target has been driven by the high SNR ratio we need to reach to precisely constrain the stellar population parameters (SNR >15 per Angstrom). More details are given in S21b.

The UVB and VIS spectra of 19 systems, these with observations completed by 2020, were released as part of the Data Release 1. In this Data Release 2, we add the UVB, VIS and NIR spectra on additional 21 new systems and the NIR spectra of the 19 galaxies released in DR1. In order to make the DR2 collection complete and self-consistent, we include here also the UVB and VIS spectra already released in DR1.

INSPIRE Data Release 2

The 21 new targets, along with their coordinates, *r*-band magnitudes (MAG_AUTO) and surface brightness are listed in Table 1. We list in the same table also the total exposure time, the Position Angle (P.A.) of the slit, the magnitude in r-band and the surface brightness profile in r-band, which have been used to determine the number of OBs for each system. Finally, we give the effective radii in arcsecond and kpc, computed as median of the quantities obtained from g,r,i-bands, and the stellar masses from SED fitting.

ID KiDS	RA (deg)	DEC (deg)	Exp.T. (sec)	P.A. (deg)	mag_r (AB)	$\langle\mu_e\rangle_r$ (AB)	$\langle R_e\rangle$ ($''$)	$\langle R_e\rangle$ (kpc)	$M_\star$ ($10^{11}M_\odot$)	SAMPLE
J0844+0148	131.0553886	+1.8132204	11240	−37.4	19.78	18.53	0.26	1.14	0.71	S20/GAMA
J0904-0018	136.0518949	-0.3054848	5620	−96.6	19.11	18.06	0.26	1.16	1.3	S20/GAMA
J0909+0147	137.3989150	+1.7880025	5620	10.3	18.68	16.05	0.30	1.05	1.05	GAMA
J0917-0123	139.2701850	−1.3887918	11240	−62.9	19.21	17.99	0.27	1.37	2.19	S20
J0920+0126	140.1291393	+1.4431610	11240	−115.6	19.52	18.82	0.33	1.51	0.98	S20/GAMA
J1026+0033	156.7231818	+0.5580979	5620	−83.1	17.39	16.98	0.34	1.02	1.48	SDSS
J1040+0056	160.2152308	+0.9407580	11240	53.4	19.52	18.85	0.31	1.29	0.93	S20
J1114+0039	168.6994335	+0.6510299	8430	34.0	19.0	17.89	0.34	1.52	1.62	S20
J1128-0153	172.0885023	−1.8890642	8430	−2.9	18.56	17.94	0.35	1.27	1.30	T18
J1142+0012	175.7023296	+0.2043419	2810	−84.8	17.02	17.90	0.71	1.40	0.84	GAMA
J1154-0016	178.6922828	−0.2779248	8430	25.4	19.52	18.28	0.22	1.06	0.64	T18/GAMA
J1156-0023	179.2186145	−0.3946597	5620	15.8	18.83	17.01	0.26	1.04	1.39	GAMA
J1202+0251	180.5132277	+2.8515452	8430	−70.6	19.43	18.53	0.31	1.49	0.68	S20
J1218+0232	184.7355807	+2.5449139	5620	1.8	19.23	18.72	0.31	1.40	0.93	S20
J1228-0153	187.0640987	−1.8989049	5620	−74.1	18.85	18.57	0.36	1.61	1.15	S20
J1411+0233	212.8336012	+2.5618381	8430	37.3	18.86	17.44	0.21	1.07	1.55	S20/GAMA
J1436+0007	219.0481314	+0.1217459	5620	−100.6	18.27	18.27	0.39	1.40	1.15	GAMA
J2202-3101	330.5472803	−31.0183808	8430	−87.6	19.43	18.77	0.31	1.45	1.10	T18
J2204-3112	331.2228147	−31.2002605	8430	−86.1	19.32	18.74	0.35	1.39	0.90	T18
J2257-3306	344.3966471	−33.1144449	8430	3.5	19.42	17.09	0.29	1.18	0.93	T18/GAMA
J2356-3332	359.1261248	−33.5334748	11240	−46.5	19.81	18.37	0.22	1.06	0.98	T18

Table 1: The INSPIRE DR2 sample. We list from left to right the galaxies' ID and coordinates, the exposure times and the position angles (along the major axis of the galaxy) of the XSH observations, the aperture magnitudes (MAG_AUTO from the KiDS DR3 catalogue, corrected for extinction), the surface brightness luminosities averaged within the effective radius ($\langle\mu_e\rangle$), both in *r*-band, the effective radii in arcsec and kpc, computed as median of the quantities obtained from g, r, i bands, and the stellar masses from SED fitting. Finally, in the last column, we list the sample from where each object was taken. For the six objects with double reference, these have been selected from T18(or S20) but then also found in the GAMA DR4.

In addition to the UVB, VIS and NIR spectra of these 21 new systems, we release as part of this DR2, the UVB, VIS and NIR spectra of the objects already publicly available from INSPIRE DR1. We remind the reader that in the previous DR, we only provided UVB and VIS, which were the arms used to constrain kinematics and stellar population parameters. Table 2 lists the DR1 objects, their coordinates and photometric and observative quantities.

ID	RA_{J2000} (deg)	DEC_{J2000} (deg)	mag_r (AB)	$\mu_{e,r}$ (AB)	OBs #	Exp.Time (sec)	P.A. (deg)	⟨SeeingUVB⟩ (arcsec)	⟨SeeingVIS⟩ (arcsec)
KiDS J0211-3155	32.8962202	-31.9279437	19.78	18.38	4/4	11240	289.3	0.88	0.85
KiDS J0224-3143	36.0902655	-31.7244923	19.25	17.98	4/4	11240	311.9	1.08	1.00
KiDS J0226-3158	36.5109217	-31.9810149	19.25	18.83	3/3	8430	33.4	0.99	0.96
KiDS J0240-3141	40.0080971	-31.6950406	19.05	17.00	2/2	5620	267.7	0.90	0.89
KiDS J0314-3215	48.5942558	-32.2632679	19.57	16.98	3/3	8430	263.4	0.74	0.71
KiDS J0316-2953	49.1896388	-29.8835868	19.66	18.09	3/3	8430	342.1	0.98	0.99
KiDS J0317-2957	49.4141028	-29.9561748	19.1	18.02	2/2	5620	339.9	0.86	0.87
KiDS J0321-3213	50.2954390	-32.2221290	19.23	18.28	4/4	11240	311.5	0.80	0.80
KiDS J0326-3303	51.5140585	-33.0540443	19.48	18.89	4/4	11240	354.4	0.90	0.90
KiDS J0838+0052	129.530452	0.88238415	19.29	19.03	3/3	8430	334.7	0.85	0.85
KiDS J0842+0059	130.666536	0.98993690	19.6	18.36	3/3	8430	346.8	0.86	0.85
KiDS J0847+0112	131.911239	1.20571289	18.41	18.69	2/2	5620	314.4	0.94	0.96
KiDS J0857-0108	134.251219	-1.14570771	19.21	19.02	2/2	2810	356.2	0.88	0.83
KiDS J0918+0122	139.644643	1.37947803	19.13	18.47	3/3	8430	301.0	0.89	0.89
KiDS J0920+0212	140.232084	2.21268315	18.87	18.54	2/2	5620	270.5	0.94	0.96
KiDS J2305-3436	346.335663	-34.6030907	19.69	18.93	4/4	11240	316.4	0.92	0.93
KiDS J2312-3438	348.238904	-34.6485914	19.32	18.34	9/9*	25290	275.4	1.40	1.33
KiDS J2327-3312	351.991016	-33.2007599	19.35	18.28	4/4	11240	315.6	0.92	0.92
KiDS J2359-3320	359.985168	-33.3335828	19.59	18.07	4/4	2810	265.1	0.90	0.87

Table 2: The INSPIRE DR1 sample. Together with ID and coordinates, we give, for each relic candidate, the aperture magnitudes (MAG_AUTO from the KiDS DR3 catalogue) and the surface brightness luminosities averaged within the effective radius ($\langle\mu_e\rangle$), both in r-band, that have been used to decide the number of OBs scheduled for each system, which is also listed in the table. For J2312-3438 a total of 4 OBs were requested, however 5 OBs were repeated because classified as grade "C" for violating the seeing constraints. This means that for this particular system we received more data than originally expected but of lower quality. Furthermore, the total exposure time on target, the Position Angle (P.A.) to which the slit was oriented, and the median seeing during observations both in UVB and VIS arm are also given. These values are the median of the headers keyword HIERARCH ESO TEL IA FWHM of each OB, representing the delivered seeing corrected per airmass. The horizontal line separates the objects that have complete observations from these only partially observed.

Data Reduction and 1D Extraction

As already explained in the INSPIRE DR1, we need to perform an ad-hoc extraction of the one 1D spectra, to take into account the fact that these galaxies are not spatially resolved and the spectra are seeing-dominated, as the effective radii of all objects on the sky are much smaller than the median seeing of the observations.

Hence, we have reduced the data using the ESO XSH pipeline (v3.5.3) under the ESO Reflex Workflow (Freudling et al., 13, version 2.11.3 only up to the creation of the 2-dimentional (2D) spectral frames (one for each arm). Subsequently we used our own Python routines, developed for S21a and already used in S21b. We cannot use ESO Internal Data Products (IDPs), as they only comprise the already extracted 1D spectra. Finally, for the VIS and NIR arms, we corrected all the spectra from telluric absorption lines using the code ‘molecfit’ (Smette et al. 2015, version 4.2) run with its interactive ESO Reflex workflow. The telluric correction has been performed with the recipe “molecfit_model” that fits telluric absorption features on telluric standard observed the same night and with the same instrument set-up of the galaxies. Once we determined the column densities of the various molecules in the spectrum, we constructed the telluric correction considering the difference in airmass between the observations of the telluric standard and the galaxy. For this purpose, we use the recipe “molecfit_calctrans”.

In the previous INSPIRE release (DR1), we have extracted and released spectra with two different approaches. On one hand, we collapsed the whole slit, but weighting more the pixels containing more flux (following the optimal extraction approach described in Naylor, 1998). On the other hand, as second approach, we also extracted the spectra of each galaxy from an aperture that contained more or less the same fraction of light for the different objects (R50, containing ~50% of the total light, but a mix from inside and outside the real effective radius). In S21b, however, we concluded that for the “relic confirmation”, the two apertures were practically equivalent. However, we note that the R50 approach is the best if we aim at comparing the INSPIRE sample with other galaxy samples from the literature, as this is the most comparable aperture, at least in terms of light fraction, to that extracted at one effective radius (Reff) for normal-size galaxies. Therefore, in this DR2, we extract spectra only following the R50 approach. The format of the spectra is described in the next Section.

Release Content

We release in this INSPIRE DR2 a total of 120 spectra on 40 galaxies (21 newly observed and 19 already given in DR1) in the UVB, VIS and NIR.

Each spectrum, in each arm and for each galaxy, is the sum of different products at the Observation Block (OB) level (from 1 to 4 OBs per system) and is released as a binary table in the FITS standard data format.

The spectra are all given at the restframed wavelength, and the redshift used is reported in the corresponding headers.

We do not join together the spectra from different arm of the same system since these have different resolution (R~3200 in UVB, R~5000 in VIS, R~4300 in NIR). However, we note that the kinematics and/or stellar population results presented in S21b and D'Ago et al. 2022 are obtained from a joint spectrum which was brought to the final resolution of FWHM = 2.52 Å, that of the single stellar population models (MIUSCAT, Vazdekis et al. 2015) used to perform the full-spectral fitting and to derive the stellar population parameters. More details on the joining procedure and the spectroscopic analysis are given in the accompanying papers. The combined and restframed version of the spectra are attached to each corresponding final science product as ancillary file, as explained below.

Data Format

1D Spectra

The spectra are stored in a FITS table which is made of a primary header (NAXIS=0) and one single extension. They all have PRODCATG=SCIENCE.SPECTRUM and are phase3 and VO compliant, they are expressed in unit of wavelength in Angstrom and Flux in erg cm^{-2} s^{-1} $Å^{-1}$. The wavelength is always measured in air for both the UVB and VIS case.

Naming convention

The names of the files all follow the same convention. They are all in the format:

"INSPIRE_<id-galaxy>_<xsh-arm>_<extraction-method>.fits"

where the id-galaxy is the one given in Table 1, but without the KiDS suffix, the xsh-arm is equal to UVB or VIS, depending on the spectrograph arm and the extraction-method is equal to R50 in this DR.

1D Ancillary spectra

To constrain the stellar population parameters with via full-spectral fitting it is desirable to a wavelength range that is large enough to break the age-metallicity Worthey et al. 1994). This is also necessary to carefully assess whether the stellar velocity dispersion measurements depend on the resolution and wavelength coverage of the spectrum used to constrain it (D'Ago et al. 2022). Thus, we first restframed and logarithmically rebinned the UVB, VIS and NIR original spectra of each object and then combined them together, also degrading their final resolution to that of the SSP mod-

els that we use in the stellar population analysis (with fix full width half maximum, FWHM = 2.52 Å). To perform the convolution, we use a Gaussian function with a variable sigma (following the prescription of Cappellari et al. 2017). More details on the procedure can be found in the papers.
The ancillary files are given as single FITS files; their naming convention is very similar to that of the main science files:
“INSPIRE_<id-galaxy>_<xsh-arm>_<resolution>_<extraction-method>.fits”
where the xsh-arm is equal to “UVB+VIS+NIR” and the resolution is “FWHM2.52”.
Each ancillary spectrum is connected to three main products (the spectra of each arm, for the corresponding galaxy), via the keyword “ASSON1” present in the primary header of each single arm spectrum.
Here below we show a typical case (J0844+0148) where we highlight the regions where the arms have been joined with yellow vertical shaded boxes, the three regions between the NIR bands with cyan boxes and the regions at the edges of the detector with orange boxes. A large value has been artificially attributed to these pixels to highlight that the data there is not trustable.

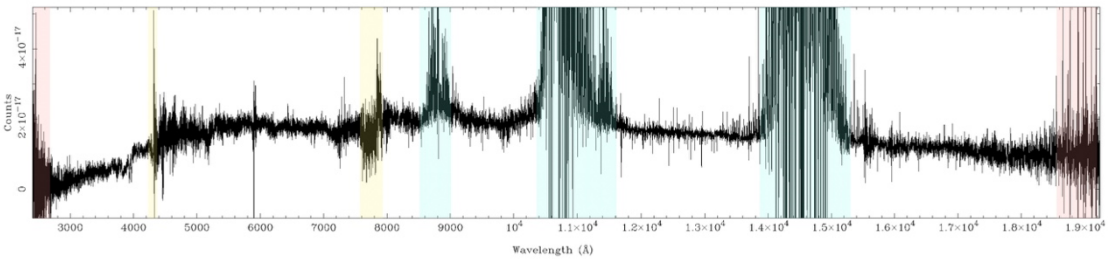

Acknowledgements

Users of INSPIRE spectra released as part of this DR2 should cite D’Ago et al. 2022, **arXiv:2302.05453**.. Users describing or using the survey in general, should instead cite the DR1 paper: Spiniello et al. 2021b, A&A, 654, A136.
Any publication making use of this data, whether obtained from the ESO archive or via third parties,
must include the following acknowledgment:

• "Based on data products created from observations collected at the European Organisation for Astronomical Research in the Southern Hemisphere under ESO programme 1104.B-0370’’

• Based on data obtained from the ESO Science Archive Facility with DOI `https://doi.org/10.18727/archive/36`

We thank the ESO Archive Science Group for the precious help they provided to make the data products presented here phase 3 compliant.

Bibliography

Bell et al., 2003, ApJS, 149, 289; Bruzual G. & Charlot S., 2003, MNRAS, 344, 1000; Buitrago et al., 2008, ApJ, 687, L61; Cappellari M., 2017, MNRAS, 466, 798; Daddi et al., 2005, ApJ, 626, 680; Ferré-Mateu et al., 2017, MNRAS, 467, 1929; Freudling, W., Romaniello, M., Bramich, D. M., et al. 2013, A&A, 559, A96; Guo et al., 2013, MNRAS, 428, 1351; Naylor, T. 1998, MNRAS, 296, 339; Oser et al., 2010, ApJ, 725, 2312; Roy et al., 2018, MNRAS, 480, 1057; Scognamiglio et al., 2020, ApJ, 893, 4; Thomas et al., 2005, ApJ, 621, 673; Tortora et al., 2018, MNRAS, 481, 4728; Tortora et al., 2016, MNRAS, 457, 2845; Trujillo et al., 2007, MNRAS, 382, 109; Trujillo et al., 2014, ApJL, 780, L20; van Dokkum et al., 2008, ApJ, 677, L5; Vazdekis et al. 2015, et al., 2015, MNRAS, 449.